But the second term in Eq. (35) must not be small. Multiplying both sides of Eq. (34) by X^tM gives

$$X^tM\bar{F}^{-1} = -(1/\varepsilon)X^t \tag{36}$$

Inserting Eq. (36) into Eq. (35) yields

$$\bar{F}^{-1} = G^+ + XX^tM\bar{F}^{-1} \tag{37}$$

i.e.,

$$G^+ = (I - XX^tM)\bar{F}^{-1} \tag{38}$$

Similarly, to avoid the calculation of $\bar{F}^{-1}$ in Eq. (38), an interim solution $\tilde{v}_j$ is first computed in Eq. (39):

$$\bar{F}\tilde{v}_j = q_j \tag{39}$$

i.e.,

$$\tilde{v}_j = \bar{F}^{-1}q_j \tag{40}$$

Embedding Eq. (37) into Eq. (40) gives

$$v_j = (I - XX^tM)\tilde{v}_j \tag{41}$$

Both Eqs. (39) and (41) are two principal formulas, as shown in Ref. 9. It is concluded that the generalized inverse technique described in this Note is also one of the DP methods as shown in Ref. 9. This is known by the fact that $MUDU^tM$ (or $MXDX^tM$) in Eq. (11) is considered as the perturbation term of DP method in Ref. 9.

VI. Numerical Results

The particular solution v_j of a numerical example shown in Ref. 8 is computed by using the GIT method in this paper and the scalar constant c_j in the general solution $y_j' = v_j + Yc_j$ of eigenvector derivatives is given by the procedure stated in Refs. 7 and 8, in which $Y = [y_1, y_2, \ldots, y_m]$. The results (general solution y_j') are the same as those of Refs. 8 and 9. In addition, to address the effect of different values of d_j, we select $d_j = d = 0.000001$, 1.0, and 100,000 ($j = 1, 2, \ldots, m$), in which $d_j = d$ means that all d_j ($j = 1, 2, \ldots, m$) are taken as a uniform value d. It is found that for very different d, the obtained solution y_j' is the same and that the particular solution v_j equals to the general solution y_j'. The former tells us that this method is numerically stable. The latter tells us that the particular solution v_j obtained by this method possibly happens to be just the general solution y_j'. Thus, it is very meaningful to propose a simple criterion by which we can know whether the v_j given by this method is y_j'. Finally, the results with $u_j = y_j$ and $u_j = x_j$ are the same.

VII. Conclusions

Based on technical analysis and numerical results, a new approach for determining the eigenvector derivatives with repeated roots has been successfully developed. This method can be applied to the calculation of eigenvector derivatives with and without repeated roots and avoids the process exerting one or m constrains to the governing equation of the eigenvector derivative. This method requires only the knowledge of the eigenvalue and its associated eigenvector under consideration. This method is numerically stable and requires no numerical convergence checks when incorporated into the existing computer program.

References

[1]Wei, F. S., "Mass and Stiffness Interaction Effects in Analytical Model Modification," *AIAA Journal*, Vol. 28, No. 9, 1990, pp. 1686–1688.

[2]Wei, F. S., "Analytical Dynamic Model Improvement Using Vibration Test Data," *AIAA Journal*, Vol. 28, No. 1, 1990, pp. 175–177.

[3]Berman, A., and Wei, F. S., "Automated Dynamic Analytical Model Improvement," NASA CR-3452, July 1981.

[4]Berman, A., Wei, F. S., and Rao, K. W., "Improvement of Analytical Models Using Modal Test Data," *Proceedings of the AIAA/ASME/ASCE/AHS 21st Structures, Structural Dynamics, and Materials Conference* (Seattle, WA), AIAA, New York, 1980, pp. 809–814.

[5]Wei, F. S., "Stiffness Matrix Correction from Incomplete Test Data," *AIAA Journal*, Vol. 18, No. 10, 1980, pp. 1274, 1275.

[6]Ojalvo, I. U., "Gradients for Large Structural Models with Repeated Frequencies," Society of Automotive Engineers, Paper 86-1789, Warrendale, PA, Oct. 1986.

[7]Mills-Curran, W. C., "Calculation of Eigenvector Derivatives for Structures with Repeated Eigenvalues," *AIAA Journal*, Vol. 26, No. 7, 1988, pp. 867–871.

[8]Dailey, R. L., "Eigenvector Derivatives with Repeated Eigenvalues," *AIAA Journal*, Vol. 27, No. 4, 1989, pp. 486–491.

[9]Zhang, D. W., and Wei, F. S., "Direct Perturbation Method for Calculation of Eigenvector Derivatives with Repeated Eigenvalues," *Journal of Solid Mechanics*, Vol. 14, No. 4, 1993, pp. 337–341.

[10]Wei, F. S., "Eigen Sensitivity Analysis with Repeated Eigenvalues," *Proceedings of 10th International Modal Analysis Conference* (San Diego, CA), 1992, pp. 596–600.

[11]Penrose, R., "A Generalized Inverse for Matrices," *Proceedings of the Cambridge Philosophical Society*, Vol. 51, 1955, pp. 406–413.

Distributed Modeling and Actuator Location for Piezoelectric Control Systems

M. Sunar*
King Fahd University of Petroleum and Minerals, Dhahran 31261, Saudi Arabia
and
S. S. Rao†
Purdue University, West Lafayette, Indiana 47907-1288

Introduction

THE piezoelectric materials have been used extensively in distributed sensing and control. Since the piezoelectric materials are distributed (not discrete) in nature, an accurate sensing and control of structures can be achieved by piezoelectric sensors and actuators.

The finite element method is a powerful technique widely used in many modern engineering design and analysis problems. Since the governing equations of piezoelectric media are complex in general, the finite element modeling suitable for the thin piezoelectric media becomes important.[1] The problem of sensor and actuator placement exists with piezoelectric sensors and actuators if they are discretely placed on various members. Hence, the issue of the piezoelectric sensor and actuator problem has been addressed[2] to see the effect of the placement on the control efficiency.

In this work, two-dimensional thin rectangular elements with pseudointernal degrees of freedom (DOF) are used to develop the finite element model of piezoelectric materials. The internal DOF are for the better representation of bending moments generated by the feedback piezoelectric voltage and are condensed to the physical nodal DOF using the Guyan reduction technique. The control efficiency effect of the location of the piezoelectric actuator pair on the beam is studied.

Finite Element Modeling of Piezoelectric Media

The quasistatic piezoelectric equations are given as[3]

$$\begin{aligned} \boldsymbol{T} &= c\boldsymbol{S} - e\boldsymbol{E} \\ \boldsymbol{D} &= e^T\boldsymbol{S} + \varepsilon\boldsymbol{E} \end{aligned} \tag{1}$$

where $\boldsymbol{T}, \boldsymbol{S}, \boldsymbol{E}$, and $\boldsymbol{D}$ are the vectors of stress, strain, electric field, and charge per unit area and c, e, and ε are the matrices of

Received Sept. 29, 1995; revision received Jan. 24, 1996; accepted for publication March 21, 1996.

*Assistant Professor, Mechanical Engineering Department.

†Professor, School of Mechanical Engineering, 1288 Mechanical Engineering Building. Member AIAA.

constitutive coefficients. The following relation is also given for the electric field in the piezoelectric media:

$$\boldsymbol{E} = -\nabla\phi \tag{2}$$

where ϕ is the electric potential. A functional Π is defined as[4]

$$\Pi = \int_V G\,\mathrm{d}V - \int_V \boldsymbol{u}^T\boldsymbol{P}_b\,\mathrm{d}V - \int_{S_1} \boldsymbol{u}^T\boldsymbol{P}_s\,\mathrm{d}S - \boldsymbol{u}^T\boldsymbol{P}_c + \int_{S_2}\phi\sigma\,\mathrm{d}S \tag{3}$$

where G is the thermopiezoelectric potential, $\boldsymbol{P}_b$ and $\boldsymbol{P}_s$ are the respective vectors of body and surface forces applied to volume V and surface S_1, $\boldsymbol{P}_c$ is the vector of concentrated forces, $\boldsymbol{u}$ is the displacement vector, and σ is the surface charge on the surface S_2. Hamilton's principle is used to obtain the finite element formulation of the piezoelectric media. The principle is expressed as

$$\delta\int_{t_1}^{t_2}(T-\Pi)\,\mathrm{d}t = 0 \tag{4}$$

where the kinetic energy T is given by

$$T = \frac{1}{2}\int_V \rho\dot{\boldsymbol{u}}^T\dot{\boldsymbol{u}}\,\mathrm{d}V \tag{5}$$

where $\dot{\boldsymbol{u}}$ is the velocity vector. Equation (4) is now written as

$$\delta\int_{t_1}^{t_2}\Pi\,\mathrm{d}t = \delta\int_{t_1}^{t_2}T\,\mathrm{d}t = -\int_{t_1}^{t_2}\int_V \rho\delta\boldsymbol{u}^T\ddot{\boldsymbol{u}}\,\mathrm{d}V\,\mathrm{d}t \tag{6}$$

upon using integration by parts with proper boundary conditions. For the thermodynamic potential G,

$$\delta G = \delta\boldsymbol{S}^T\boldsymbol{T} - \delta\boldsymbol{E}^T\boldsymbol{D} \tag{7}$$

For the finite element formulation, the rectangular elements ($2a\times 2b$) with pseudointernal DOF are used to better represent the bending moments caused by the piezoelectric actuator. The term N_i ($i = 1,\ldots,4$) is the ith shape function used for the rectangular elements, and the other two shape functions for the pseudointernal DOF are given as

$$N_5 = 1-(x^2/a^2), \qquad N_6 = 1-(y^2/b^2) \tag{8}$$

which vanish at the element boundaries where $x = \pm a$ and $y = \pm b$. Applying the finite element method to Eq. (4) yields the following piezoelectric equations (after assemblage):

$$\begin{bmatrix} M_{uu} & 0 \\ 0 & 0 \end{bmatrix}\begin{Bmatrix} \ddot{\boldsymbol{u}} \\ \ddot{\phi} \end{Bmatrix} + \begin{bmatrix} K_{uu} & K_{u\phi} \\ K_{\phi u} & -K_{\phi\phi} \end{bmatrix}\begin{Bmatrix} \boldsymbol{u} \\ \phi \end{Bmatrix} = \begin{Bmatrix} \boldsymbol{F} \\ \boldsymbol{G} \end{Bmatrix} \tag{9}$$

where the Guyan static model reduction technique is used to condense the pseudointernal DOF to the physical nodal DOF. In Eq. (9), $\boldsymbol{u}$, ϕ, $\boldsymbol{F}$, and $\boldsymbol{G}$ are the global nodal displacement, electric potential, force, and applied charge vectors, respectively. The element matrices and vectors in Eq. (9) are found as

$$[M_{uu}]_{\mathrm{el}} = \int_{V_{\mathrm{el}}}\rho N_u^T N_u\,\mathrm{d}V, \qquad [K_{u\phi}]_{\mathrm{el}} = \int_{V_{\mathrm{el}}} B_u^T e B_\phi\,\mathrm{d}V$$

$$[K_{uu}]_{\mathrm{el}} = \left[\int_{V_{\mathrm{el}}} B_u^T c B_u\,\mathrm{d}V\right] - \left[\int_{V_{\mathrm{el}}} B_u^T c Y\,\mathrm{d}V\right] \times \left[\int_V Y^T c Y\,\mathrm{d}V\right]^{-1}\left[\int_{V_{\mathrm{el}}} B_u^T c Y\,\mathrm{d}V\right]^T \tag{10}$$

$$[K_{\phi\phi}]_{\mathrm{el}} = \int_{V_{\mathrm{el}}} B_\phi^T\varepsilon B_\phi\,\mathrm{d}V, \qquad \boldsymbol{G}_{\mathrm{el}} = \int_{(S_2)_{\mathrm{el}}} N_\phi^T\sigma\,\mathrm{d}S$$

$$\boldsymbol{F}_{\mathrm{el}} = \int_{V_{\mathrm{el}}} N_u^T\boldsymbol{P}_b\,\mathrm{d}V + \int_{(S_1)\mathrm{el}} N_u^T\boldsymbol{P}_s\,\mathrm{d}S + N_u^T\boldsymbol{P}_c$$

where N_u and N_ϕ are the shape function matrices for displacement and electric fields and B_u and B_ϕ are defined for each element as

$$B_u = [L_u \quad N_u], \qquad B_\phi = [\nabla N_\phi] \tag{11}$$

where L_u is the differential operator that relates strain to displacement in two dimensions. In Eq. (10), X and Y matrices are given for each element as

$$X = \begin{bmatrix} 0 & 0 \\ N_5 & N_6 \end{bmatrix}, \qquad Y = [L_u X] \tag{12}$$

Effect of Piezoelectric Actuator Location in Active Control

A cantilever beam having a piezoelectric actuator pair at the top and bottom surfaces is considered as a system to investigate the effect of distributed piezoelectric actuator location in active vibration control. The sensed signals are fed to the piezoelectric pair according to the control law implemented. The linear quadratic regulator (LQR) scheme is employed as the control law to determine the control gains necessary for adjusting sensory signals. The equations of motion of the system are converted to the standard state–space form as

$$\dot{z} = Az + B\boldsymbol{u}_G \tag{13}$$

Equation (9) can be written in the form of Eq. (13) with

$$z = \begin{Bmatrix} \boldsymbol{u} \\ \dot{\boldsymbol{u}} \end{Bmatrix}, \qquad \boldsymbol{u}_G = \boldsymbol{V} = (1/c_p)\boldsymbol{G}$$

$$A = \begin{bmatrix} 0 & I \\ -M_{uu}^{-1}K_n & 0 \end{bmatrix}, \qquad B = \begin{bmatrix} 0 \\ M_{uu}^{-1}D \end{bmatrix} \tag{14}$$

where

$$K_n = K_{uu} + K_{u\phi}K_{\phi\phi}^{-1}K_{\phi u}, \qquad D = c_p K_{u\phi}K_{\phi\phi}^{-1} \tag{15}$$

and c_p is the capacitance. According to the LQR scheme, the control input vector $\boldsymbol{u}_G$ is chosen of the form

$$\boldsymbol{u}_G = -K_G z \tag{16}$$

so that the performance index

$$J = \int_0^\infty \left(z^T Q z + \boldsymbol{u}_G^T R\boldsymbol{u}_G\right)\mathrm{d}t \tag{17}$$

with respective positive semidefinite and positive definite weighting matrices of Q and R is minimized. The scheme yields the gain matrix K_G to be

$$K_G = R^{-1}B^T P \tag{18}$$

where P is given by the algebraic Riccati equation

$$PA + A^T P - PBR^{-1}B^T P + Q = 0 \tag{19}$$

In this research study, the location of the piezoelectric actuator pair is varied along the cantilever beam to see the impact of piezoelectric actuator location on the vibration control efficiency of the closed-loop system. The closed-loop system here refers to the cantilever beam controlled by the piezoelectric actuator. For the control efficiency, the absolute sum of the tip deflections of the closed-loop system subjected to some disturbance within a time interval is taken as objective. The magnitude of this objective is computed for different actuator locations. When the magnitude of this objective is less at a certain actuator location, say at d_1, compared with another location, say at d_2, it is decided that the actuator pair at location d_1 is more effective than that at d_2.

Numerical Results

The cantilever beam with piezoelectric actuator pair shown in Fig. 1 is used to illustrate the procedure just outlined. The piezoelectric material is taken as polyvinylidene fluoride (PVDF), and the beam is made of aluminum. The material properties of PVDF are $c_{11} = 3.8 \times 10^9$ Pa, $e_{31} = 0.046$ C/m^2, $\varepsilon_{33} = 1.062 \times 10^{-10}$ F/m, $c_p = 3.8 \times 10^{-6}$ F, and $\rho = 1800$ kg/m^3; those of aluminum are $c_{11} = 7.3 \times 10^{10}$ Pa, $\rho = 2750$ kg/m^3, and $\nu = 0.33$. The heights of the beam and piezoelectric actuators are taken as $h_b = 6$ and 0.6 mm. The depth of both beam and piezoelectric actuators is $w = 6$ mm, and the length of the beam is $L = 60$ mm. The length of both piezoelectric actuators is assumed as $L/2$.

The closed-loop structure controlled according to the LQR scheme is subjected to a unit step force at the tip in the y direction, and the simulation results are given in Figs. 2 and 3. Figure 2 shows the tip deflection (tip displacement in the y direction) of the beam for two different actuator locations, whereas Fig. 3 shows the absolute sum of the tip deflections of the beam in the given time interval (the sum is found by adding the absolute magnitudes at every 0.001 s). The Q and R matrices for the LQR method are taken as $0.001 \times I$ and I, where I is the identity matrix with proper dimensions. Other Q and R matrices can be used equally well. It is evident from the results, especially in Fig. 3, that the piezoelectric actuator pair closer to the fixed end is more effective in attenuating structural vibrations than the pair further away from the fixed end.

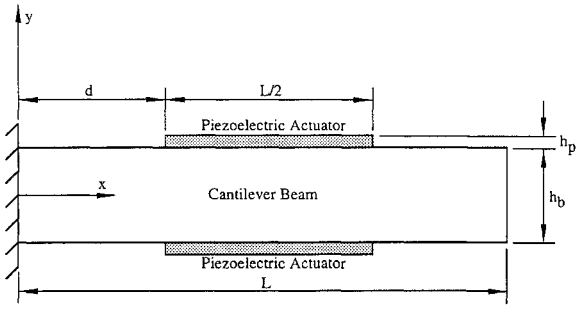

Fig. 1 Cantilever beam with piezoelectric actuator pair (not to scale).

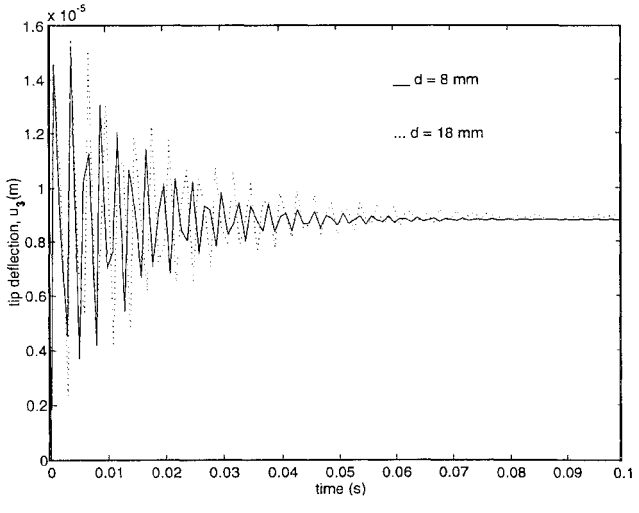

Fig. 2 Vibrational tip deflection of closed-loop system.

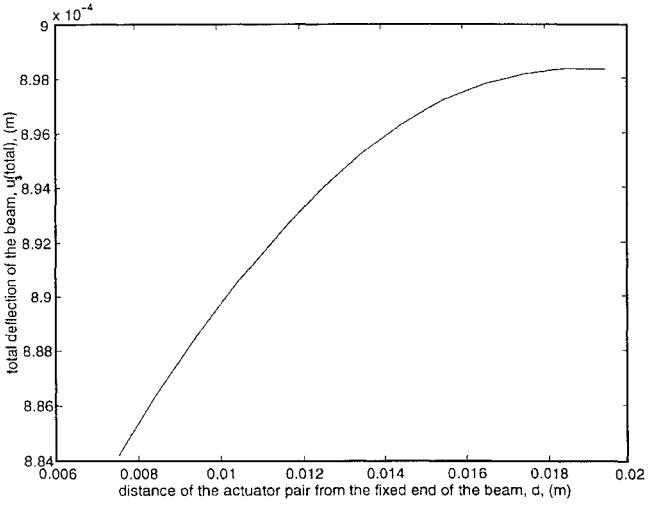

Fig. 3 Absolute sum of vibrational tip deflections of closed-loop system from 0 to 0.1 s.

Conclusion

Observing the magnitude of structural vibrations, the piezoelectric actuator pair closer to the fixed end of the cantilever beam is more efficient than the pair further away from the fixed end. This result is important in piezoelectric actuator placement for structures that can be modeled as cantilever beams. The procedure outlined in this Note can be generalized to more complicated systems.

Acknowledgment

The first author acknowledges the support provided by King Fahd University of Petroleum and Minerals for this research.

References

[1]Rao, S. S., and Sunar, M., "Analysis of Thermopiezoelectric Sensors and Actuators in Advanced Intelligent Structural Design," *AIAA Journal*, Vol. 31, No. 7, 1993, pp. 1280–1286.

[2]Soderkvist, J., "Dynamic Behavior of a Piezoelectric Beam," *Journal of the Acoustical Society of America*, Vol. 90, No. 2, 1991, pp. 686–692.

[3]Tiersten, H. F., *Linear Piezoelectric Plate Vibrations*, Plenum, New York, 1969.

[4]Nowacki, W., "Some General Theorems of Thermopiezoelectricity," *Journal of Thermal Stresses*, Vol. 1, No. 2, 1978, pp. 171–182.

Practical Complete Modal Space and Its Applications

De-Wen Zhang*
Beijing Institute of Structure and Environment Engineering, Beijing, People's Republic of China
and
Fu-Shang Wei†
Kaman Aerospace Corporation, Bloomfield, Connecticut 06002

I. Introduction

THE modal expansion method has been used in many important subjects, such as dynamic response, substructural modal synthesis, calculation of eigenvector derivatives, model correction, and reduction of dynamic models. In using the modal expansion technique, there exists numerical error as a result of truncation of modes, and the precision of the results sometimes is poor. To reduce the error of truncated modes, the development of a practical complete modal space (PCMS) method is necessary and strongly recommended.

The PCMS method was first applied to the correction of structural dynamic models.[1–4] Later, it was successfully used in the calculation of the eigenvector derivatives with repeated frequencies,[5] in the development of an accurate modal synthesis,[6–9] in the reduction of dynamic models,[10,11] and in the medium substitution problems for

Received May 2, 1995; revision received March 25, 1996; accepted for publication March 26, 1996.

*Senior Research Engineer, First Research Division, P.O. Box 9210. Member AIAA.

†Principal Engineer, Engineering and Development Department. Senior Member AIAA.